



Superfilling When Adsorbed Accelerators Are Mobile

D. Josell,^z T. P. Moffat,* and D. Wheeler*

National Institute of Standards and Technology, Metallurgy Division of the Materials Science and Engineering Laboratory, Gaithersburg, Maryland 20899, USA

Bottom-up superconformal feature filling during electrodeposition, called “superfilling,” that is used for industrial processing of damascene copper interconnects has also been demonstrated during electrodeposition of silver and gold. The curvature enhanced accelerator coverage (CEAC) mechanism has been proposed to underlie all three processes and has been used to quantitatively predict observed filling of patterned features. The key feature of the CEAC mechanism is redistribution of adsorbed additives through changes of local surface area as dictated by mass conservation and the relative strengths of adsorption. Previous studies of CEAC-mediated superfilling have neglected adsorbate diffusion along the surface that might arise during deposition due to the CEAC-induced gradients in surface coverage. This paper extends the CEAC model to include such diffusion, applying the resulting formulation to understand differences in the geometries of experimental superfilling systems.
© 2007 The Electrochemical Society. [DOI: 10.1149/1.2434684] All rights reserved.

Manuscript received September 29, 2006. Available electronically February 6, 2007.

Bottom-up deposition in fine trenches, called “superfilling,”¹ underlies industrial processing of damascene copper interconnects for microelectronics. The process, which occurs during electrodeposition in electrolytes containing specific combinations of additives, has also been demonstrated during electrochemical deposition (ECD) of silver²⁻⁶ and gold^{7,8} (see Fig. 1), as well as during additive-accelerated chemical vapor deposition (CVD) of copper.⁹⁻¹⁴ Several mechanisms have been invoked to explain the superfill process during Cu ECD. These include variations of the traditional leveling model that presumes depletion of a deposition rate suppressing additive within the filling feature,^{1,15-17} models that invoke equilibrium with competitive adsorption of accelerating and suppressing additives,¹⁸ models that relate area change to the changing coverage of accelerating and suppressing adsorbates in combination with equilibrium-like relationships,¹⁹ and models that relate area change to the changing coverage of accelerating adsorbates that either accumulate under interface or transport limits or are adsorbed prior to metal deposition.^{20,21} These last models, based on the curvature enhanced accelerator coverage (CEAC) mechanism, predict that an electrolyte-additive system can yield superfill if the additive accelerates the deposition rate when it adsorbs on the deposit surface and remains on the surface during deposition. Under these circumstances the CEAC mechanism predicts that the decreasing area of the metal surface at the bottoms of filling features will lead to locally increasing coverage of the adsorbed accelerator, which will lead to increased local deposition rate and bottom-up, superconformal growth (superfilling). CEAC models use only kinetics obtained from studies on planar substrates; no additional parameters are used for simulating feature filling or more general interface evolution.

Superfilling is distinct from “leveling” that arises from, e.g., spatially varying suppression due to a (consumption-induced) vertical gradient of rate-suppressing additive within the electrolyte in the filling feature. Although such a process has recently been described for Au deposition in micrometer-size trenches,²² leveling is typically associated with larger length scales because of the underlying diffusion-consumption balance for the additive within the electrolyte. Leveling-induced superconformal deposition processes do not exhibit desirable accelerated upward motion of a flat bottom within the filling feature or undesirable formation of a bump over the filled feature, both traditional hallmarks of superfilling processes.

CEAC-based models quantitatively predict the evolving shape of the growth front in superfilling features for Cu,^{20,21,23} Ag,^{2,4} and Au⁸ superfill by ECD as well as Cu^{12,13} superfill by CVD. As shown in Fig. 2, CEAC models predict the bottom-up filling of Fig. 1 as well as bumps observed over superfilled features.^{3,13,20,23} They also predict the inception of deposition at the lower corners of the filling

feature; associated discontinuities of the surface slope such as the right angle between the sidewalls and bottom surface shown during bottom-up filling are visible in the simulations of Fig. 2. The predicted deposition, beginning at the lower corners and followed by bottom-up growth from the resulting “corner” on the midline of the trench, also capture experimental results during concurrent catalyst accumulation and Cu deposition (Fig. 3a); the experimental surface exhibits all the discontinuities of slope found in the prediction and experiment for preadsorbed catalyst (Fig. 1a and 2). In contrast, the surfaces of the Au deposit in Fig. 1c are rounded; there are no discontinuities of slope. The Ag geometry exhibits rounded bottoms as deposition progresses (Fig. 1b); results for Ag deposition with concurrent catalyst accumulation (Fig. 3b) also exhibit rounding rather than sharp corners.

It has been suggested that rounding of the Au deposit at the bottoms of the filling trenches might be due to diffusion of adsorbed accelerator along the surface during filling.⁸ Such a proposal is not unreasonable in light of the comparatively long deposition times and small feature sizes, as well as the high mobility that might be expected for the low coverage of an underpotential-deposited metal such as the Pb accelerator. This work seeks to quantify the impact of such adsorbate diffusion on superfilling processes. The analysis is done in the context of the CEAC mechanism of superconformal film growth.

Implementing Surface Diffusion in the CEAC Mechanism

Quantitative modeling of superfill through the CEAC mechanism requires establishing the forms and parameters of two principal equations. The first equation quantifies the relationship between adsorbate coverage and metal deposition rate (i.e., current density in electrodeposition). The second equation quantifies the change of the adsorbate coverage in terms of the evolution of the deposit geometry. With boundary conditions derived from consistency of metal and adsorbate accumulation at the deposit surface with transport from the electrolyte, these two equations allow for quantitative prediction of feature filling.

A linear form is used for the deposition rate-adsorbate coverage relationship

$$v(\theta) = A + B\theta \quad [1]$$

where θ is the coverage of adsorbed accelerating additive and cannot exceed unity. General Butler-Volmer relationships for the current (metal deposition rate) on surfaces with multiple adsorbates can be expressed in this form as long as the deposition rate is linear in the coverages of the adsorbates. Although not stated explicitly in this form, the deposition rate is typically presumed to scale with the

* Electrochemical Society Active Member.

^z E-mail: Daniel.josell@nist.gov

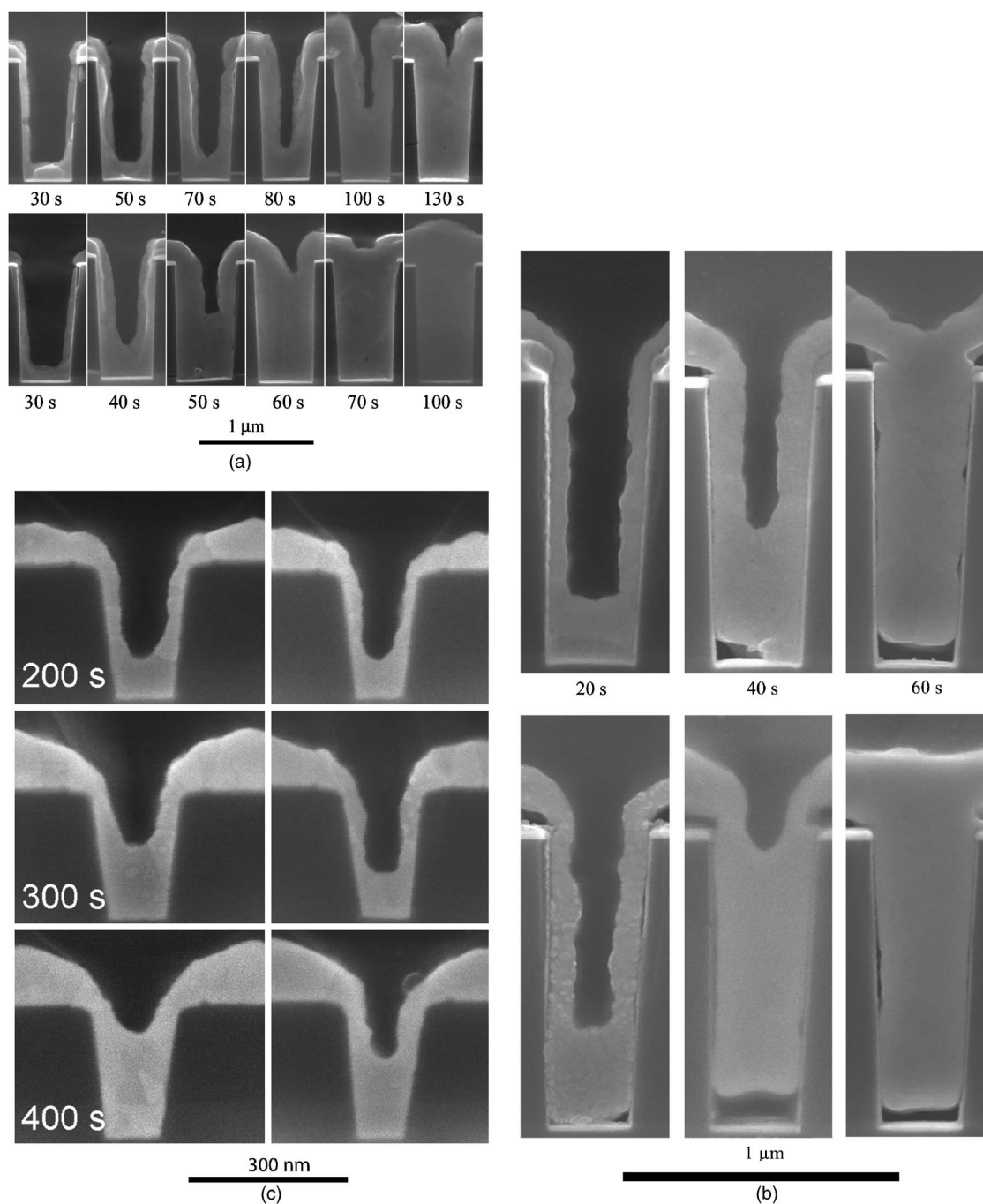


Figure 1. Images of (a) copper, (b) silver, and (c) gold superfill. The copper superfill is excerpted from Fig. 8 of Ref. 23; it shows filling of trenches with two different adsorbate coverages (upper/lower row) as functions of deposition time. The silver superfill is excerpted from Fig. 2 of Ref. 5; it shows filling of trenches with two different adsorbate coverages (upper/lower row) as functions of deposition time. The gold superfill is excerpted from Fig. 5 of Ref. 8; it shows filling of two trenches of different width (left/right column) as a function of deposition time. The Cu filling sequences are characterized by sharp corners and straight edges. The Ag filling sequences exhibit corners at the earliest time, with rounding evident in subsequent images. The Au filling sequences show substantial rounding at all times. Details concerning the processing of the specimens can be found in the respective references.

concentration of the metal ion in the adjacent electrolyte. While the deposition rate can be explicitly stated in terms of concentration fields as a function of position within the filling feature,^{8,20,23,24} for submicrometer-size features the concentration generally differs little from that at the top of the feature. For most of this evaluation it is assumed that the concentration of metal ion within the filling feature is uniform, being related to the bulk concentration by diffusional transport across the boundary layer; the parameters A and B for Eq. 1 are obtained from the deposition kinetics multiplied by the scaled

metal ion concentration thus obtained for disclosed superfilling processes. For Au filling modeled in this study, metal ion depletion reduces A and B of Eq. 1 by only a few percent from their interface kinetic limited values because the deposition rates considered are well below the maximum rate possible at the transport limit of the Au ions in solution. On the other hand, A and B for Cu filling are reduced by a factor of 2, as the associated deposition rates are approximately half the transport limit in the steady state.

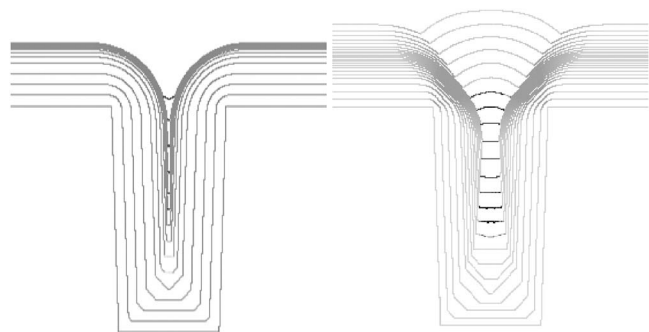


Figure 2. CEAC predictions of superfill. The simulations are excerpted from Fig. 9 of Ref. 23; the left (right) simulation corresponds to the upper (lower) filling sequence in Fig. 1a. The modeling conditions can be found in the referenced work. Gray scale is indicative of coverage of adsorbed accelerator (darker for higher coverage), except where crowding of contours leads to unintentional contrast.

The equation describing the evolution of adsorbate coverage on the moving surface is written

$$\frac{d\theta}{dt} = \kappa v \theta + D \frac{\partial^2 \theta}{\partial s^2} \quad [2]$$

The first term on the right side imposes mass conservation when area changes through motion of the interface; it expresses the normalized rate of area change in terms of the local curvature κ and the normal velocity v , thereby accounting for compression or dilation of the adsorbate coverage during deposition on nonplanar surfaces ($\kappa \neq 0$). This term underlies the superfill phenomenon and gives the curvature-enhanced accelerator coverage mechanism its name. The second term is newly introduced and accounts for diffusion of adsorbate along the surface arising from gradients of coverage along

the surface. It is derived by assuming that the flux of adsorbate along the surface (position defined by the arclength s) is proportional to the gradient of coverage (i.e., Fickian diffusion), and the divergence of the flux yields the rate of accumulation; the proportionality constant is the diffusion coefficient D . This expression is appropriate for a geometry that can be solved in two-dimensional form, e.g., a trench; it would be replaced by $D\nabla_s^2\theta$, where ∇_s^2 is a Laplacian operator on the surface, for general three-dimensional geometries.

Equation 2 does not include terms for accumulation and consumption of the accelerating adsorbate that are found in many previously published CEAC models. Accumulation is ignored in this work, as it models experiments with substrates “derivatized” with accelerator prior to metal deposition, consistent with the experimental processes for the Cu, Ag, and Au superfill in Fig. 1; there is no accelerator in the electrolyte for accumulation during the metal deposition process. The utility of this approach for understanding and improving superfilling has been demonstrated previously for electrodeposition of Cu, Ag, and Au and chemical vapor deposition of Cu. Consumption is ignored because its impact on filling geometry is generally small under conditions where the superfill dynamic is dominant. The derivatization process permits superfill to commence immediately upon the start of metal deposition, without an “incubation period” of conformal growth, and allows filling of higher aspect ratio features than can be filled if accelerator and metal accumulate simultaneously.²⁴ Expressions for accumulation and/or consumption can be added to the right side of Eq. 2 if their inclusion is desired.

Modeling and Experimental Results

Superfill of a trench of width w and height h was modeled using Eq. 1 and 2 assuming uniformly distributed accelerator coverage θ_0 at the start of metal deposition. The results are plotted for nondimensional combinations of variables to increase their generality. To obtain these combinations, Eq. 1 and 2 were nondimensionalized by

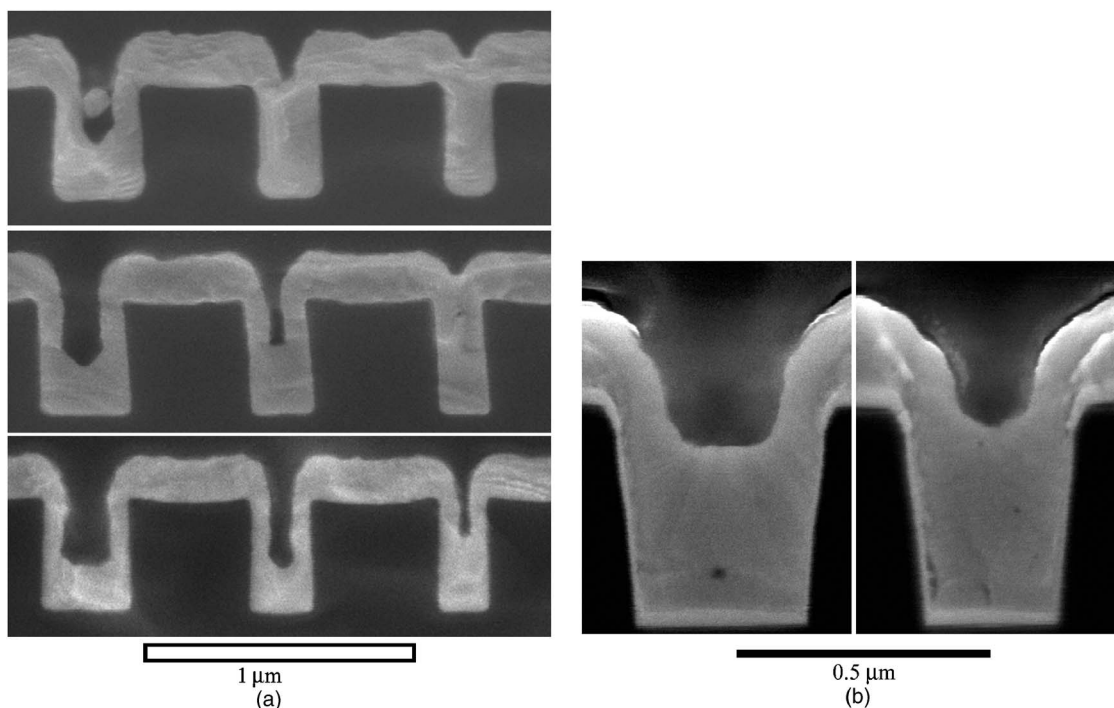


Figure 3. Images excerpted from (a) Fig. 10 of Ref. 23, showing sequential superfilling of trenches during Cu deposition concurrent with accelerator accumulation, and (b) Fig. 8 of Ref. 4, showing partially filled vias from Ag deposition concurrent with accelerator accumulation. Note the sharp corners associated with the Cu superfill process vs the rounding where the sidewalls meet the bottom surface of the Ag-filled feature. Processing conditions can be found in the source publications.

Table I. Parameters for Cu superfill in Fig. 1a; coverage and kinetics from Fig. 9 and Table II, respectively, of Ref. 23. Kinetics for the suppressed surface are those for the “relaxed” case (i - η value). The coverage corresponds to that for the bottom filling sequence in Fig. 1a. Values of both A and B are reduced by a factor of two from values obtained from kinetics in Ref. 23 because of metal ion depletion expected at the surface during deposition on a planar substrate.

θ_0	0.054
$A, \mu\text{m/s}$	7.2×10^{-4}
$B, \mu\text{m/s}$	3.9×10^{-2}
$w, \mu\text{m}$	0.5
$h, \mu\text{m}$	1.0

scaling all dimensions by the trench width w , scaling growth velocity by that associated with deposition on the planar surface with the initial accelerator coverage θ_0 , i.e., scaling by $v_0 = A + B\theta_0$, and scaling time by the ratio w/v_0 . This yields the following definitions of the dimensionless variables

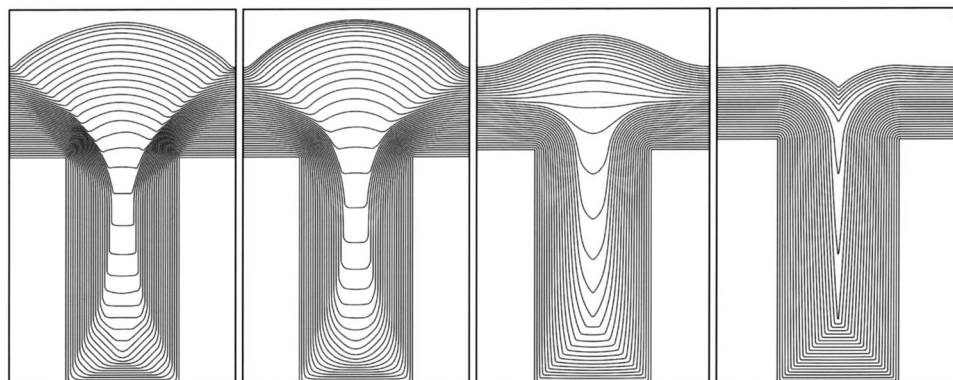
$$\begin{aligned}
 w &\equiv \bar{w}w \rightarrow \bar{w} = 1 \\
 h &\equiv \bar{h}w \\
 \kappa &\equiv \bar{\kappa}/w \\
 s &\equiv \bar{s}w \\
 v &\equiv \bar{v}(A + B\theta_0) \equiv \bar{v}v_0 \\
 t &\equiv \bar{t}w/v_0
 \end{aligned} \quad [3]$$

where the dimensionless variables have the bars over them. The adsorbate coverage θ is already dimensionless, being equal to the ratio of actual coverage and the maximum possible coverage (i.e., one monolayer or some fraction thereof).

With the definitions found in Eq. 3, the deposition rate-coverage relationship in Eq. 1 becomes

Table II. Parameters for Au superfill shown in Fig. 1c; coverage and kinetics from Ref. 8. The width is that of the wider trenches (left side of Fig. 1c) at midheight.

θ_0	0.15
$A, \mu\text{m/s}$	4.8×10^{-5}
$B, \mu\text{m/s}$	9.8×10^{-4}
$w, \mu\text{m}$	0.15
$h, \mu\text{m}$	0.3



$$\bar{v} = 1 + \frac{\theta - \theta_0}{A/B + \theta_0} \quad [4]$$

The adsorbate evolution expression in Eq. 2 becomes

$$\frac{d\theta}{d\bar{t}} = \bar{\kappa}\bar{v}\theta + \frac{D}{w(A + B\theta_0)} \frac{\partial^2 \theta}{\partial \bar{s}^2} \quad [5]$$

for filling of a trench of width $\bar{w} = 1$ and height $\bar{h} = h/w$ with initial accelerator coverage θ_0 . There are four dimensionless quantities required to fully define the dimensionless problem: the trench aspect ratio h/w , the initial adsorbate coverage θ_0 , and the ratios A/B and $D/w(A + B\theta_0)$, the last of which can be written shorthand as D/wv_0 . The inverse of the ratio A/B conveys the impact of changing adsorbate coverage on the deposition rate given starting coverage θ_0 ; Tables I and II, obtained from kinetics disclosed for Cu²³ and Au superfilling electrolytes, yield B/A of 54 for Cu and 20 for Au (current industrial Cu superfilling electrolytes likely exhibit a higher B/A ratio). The ratio D/wv_0 reflects the relative impacts of surface diffusion and area change and is the focus of this work. Specification of two additional parameters, e.g., w and A , permits modeling of absolute length and time scales of the six-parameter ($h, w, \theta_0, A, B,$ and D) fully dimensional problem if such is desired.

Figure 4 shows simulations for the parameters in Table I, which are appropriate for the Cu superfill in the second row of Fig. 1a. Simulations are shown for values of D/wv_0 where insignificant diffusion occurs during feature filling ($D/wv_0 = 0.01$), consistent with previous CEAC modeling, through filling that is nearly dominated by surface diffusion ($D/wv_0 = 10$) for which the solution is approaching conformal filling as surface diffusion overwhelms the ability of area change to nonuniformly redistribute adsorbed accelerator. For the parameters in Table I, the modeled D/wv_0 values correspond to surface diffusion coefficients D for the accelerator ranging from 10^{-13} cm²/s to 10^{-10} cm²/s.

Figure 5 shows simulations for the parameters in Table II, appropriate for the Au superfill in the wider trench of Fig. 1c. Taking account of the smaller w and v_0 values, the values of D are more than an order of magnitude smaller than those for the simulations in Fig. 4 with the same D/wv_0 , i.e., surface diffusion is predicted to become significant at a smaller value of D for the Au system operated under the given deposition conditions.

Surface diffusion of the adsorbed accelerator, by reducing spatial gradients of adsorbate coverage, works against the CEAC-induced variations that underlie superfill. Comparison of the growth contours in Fig. 1a (and Fig. 3a) with the simulations of Fig. 4 indicates that $D/wv_0 < 0.01$ for the Cu superfilling system. Using the feature dimensions and deposition kinetics summarized in Table I, this yields an upper bound of $D < 10^{-13}$ cm²/s for diffusion of the adsorbed Na₂[SO₃(CH₂)₃S]₂ (SPS) accelerator on the deposit surface in the cited Cu superfill experiments. Based on the modeling results, it will

Figure 4. Predicted Cu superfilling of a trench of aspect ratio 2 for parameters from Table I and dimensionless diffusion coefficient D/wv_0 (left to right): 0.01, 0.1, 1.0, and 10. Small but nonzero D/wv_0 results in rounding of the corners, while intermediate values cause cusplike filling similar to that typical of leveling. Filling is nearly conformal at the highest D/wv_0 value.

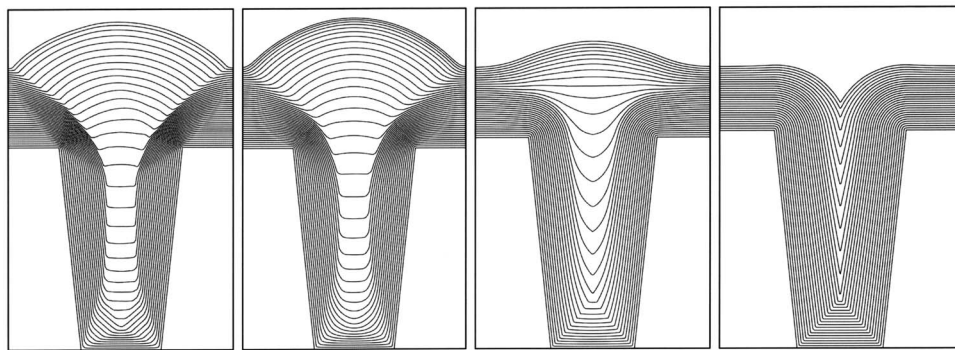


Figure 5. Predicted Au superfilling of a trench of aspect ratio 2 (based on trench width at midheight) for parameters from Table II and dimensionless diffusion coefficient D/wv_0 (left to right): 0.01, 0.1, 1, and 10. Small but nonzero D/wv_0 results in rounding of the corners, while intermediate values cause cusplike filling similar to that typical of leveling. Filling is nearly conformal at the highest value of D/wv_0 ; filling by geometrical leveling continues indefinitely as D/wv_0 increases because of the 6° tilt of the sidewalls (chosen to be consistent with the experimental images in Fig. 1c).

take substantially smaller features (w) to make surface diffusion significant for this electrolyte-adsorbate system (D) and deposition rate (v_0).

The curved bottom-to-cusp-like filling predicted in Fig. 4 for D/wv_0 in the range from 0.1 to 1 (for which adsorbate diffusion is becoming significant) resembles the Ag filling geometries of Fig. 1b at intermediate times (and Fig. 3b). This suggests that diffusion of the adsorbed Se accelerator in the Ag superfilling system is substantial for the experimental conditions used. While the modeled kinetics are not those for the Ag filling (for which a robust kinetic description is not available), the similarity of feature size and filling time with the lower Cu fill sequence in Fig. 1a suggests use of the kinetics and coverage listed in Table I. Using $w = 0.3 \mu\text{m}$ (from Fig. 1b) with the kinetics and coverage from Table I and D/wv_0 of order 0.1–1.0 yields D of the adsorbed accelerator of order 10^{-12} – $10^{-11} \text{ cm}^2/\text{s}$ for the conditions studied. The limited spatial extent of the rounded corners and remaining flat bottom of the via filled with Ag using concurrent Se accelerator accumulation shown in Fig. 3b suggest that surface diffusion is just becoming significant for these deposition conditions; the rounding limited to corners is similar to that shown in Fig. 4 for $D/wv_0 = 0.1$ (surface diffusion just becoming significant), albeit the simulation is for a different geometry and materials system.

Comparison of the rounded bottoms of the growth contours in the Au superfill of Fig. 1c with the simulations in Fig. 5 suggests D/wv_0 of the adsorbed accelerator is also of order 0.1–1.0. Using the feature dimensions and deposition kinetics in Table II, this suggests that D is of order 10^{-14} – $10^{-13} \text{ cm}^2/\text{s}$ for the adsorbed Pb accelerator in the Au superfill experiments; this value is smaller than that determined for the Ag case because v_0 for the Au is smaller (manifesting in substantially longer deposition times) as is w . Based on Fig. 5, if higher deposition rates could be achieved, surface contours would be expected to show the sharp corners exhibited by the Cu superfilling system.

Figure 6 uses the Cu deposition kinetics in Table I to examine the impact of surface diffusion on the maximum aspect ratio of trenches that can be successfully filled. Specifically, Fig. 6 indicates whether the deposit on the bottom surface reaches the height of the patterned trench before the deposits on the sidewalls impinge there. Because superfill through the CEAC mechanism derives from increased accelerator coverage on the bottom surface of the filling feature, one might expect that transfer of accelerator back to the sidewalls by surface diffusion would always be detrimental to superfill. However, the nonzero diffusion of adsorbed accelerator also leads to deposition rates increasing down the sidewalls so that angled sidewall deposits develop even in trenches with vertical sidewalls, and geometrical leveling through “zipping” up of the feature facilitates filling of higher aspect ratio features. This effect is evident in Fig. 7, which shows the simulations corresponding to filling of a trench of aspect ratio 4 for four different values of D/wv_0 (values indicated on Fig. 6 by black dots). Limited diffusion of the adsorbed accelerator is thus predicted to be quite beneficial.

The variable thickness of the sidewall deposits predicted for su-

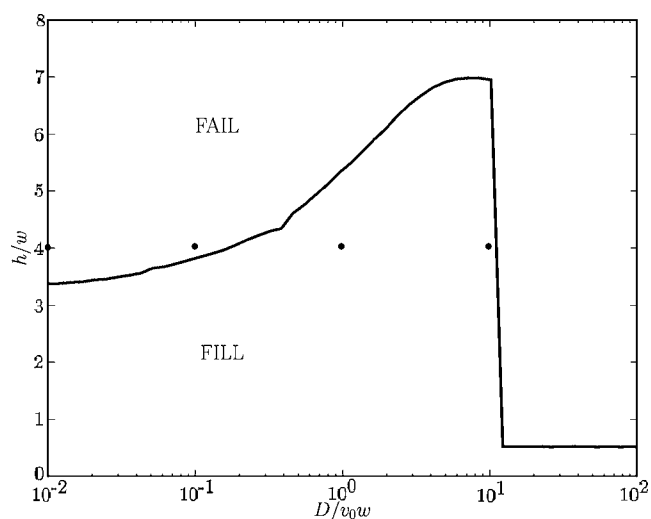


Figure 6. The maximum aspect ratio compatible with seam-free trench filling for kinetics of Cu superfilling from Table I is indicated as a function of the dimensionless diffusion coefficient D/wv_0 . All other parameters are held constant. Limited mobility of the adsorbate is seen to improve filling; it does so by creating tilted deposits on the sidewalls that permit geometrical leveling. Fine features along the curve are artifacts of resolution-induced uncertainty in the filling simulations.

perfilling processes with moderately mobile adsorbates (see, e.g., Fig. 4 and 5 for D/wv_0 of order unity) resembles that typical of deposition in leveling systems. The similarity is coincidental; the thickness variation in leveling occurs because the concentration gradient of deposition rate-suppressing leveler within the feature induces spatially varying coverage of adsorbed suppressor as opposed to the spatially varying coverage of adsorbed accelerator that results from the interplay of surface diffusion and the CEAC mechanism in this work. The bump that forms over features after superfilling is also predicted to shrink with increasing mobility of the adsorbed accelerator (Fig. 4 and 5), substantially reducing, even eliminating, what is frequently the only post-facto evidence that a feature was filled by a superfilling process.^a In light of this “blurring” of the line between the geometries of features that have been filled by superfilling vs leveling processes, experimental studies should include time-dependent filling to provide evidence to support statements of

^a Area decreases more rapidly within filling vias than within filling trenches under the same deposition conditions; one might therefore expect via filling to maintain CEAC induced effects such as bump formation over a correspondingly wider range of conditions. In fact, the only overfill bumps observed in silver (or gold) superfilling studies were found over Ag filled vias (Fig. 3 of Ref. 3 and Fig. 7 of Ref. 4).

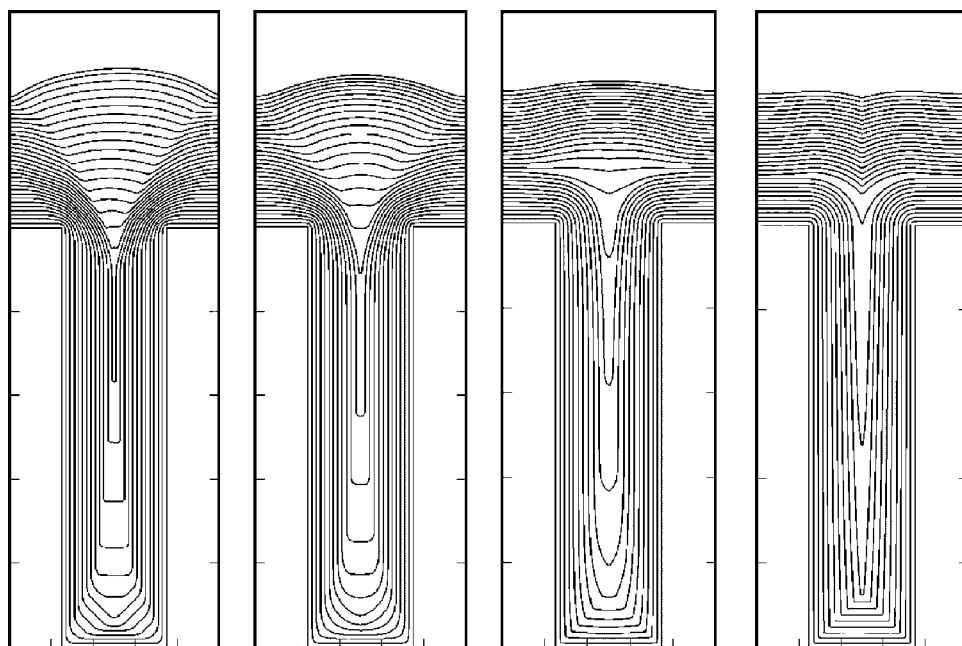


Figure 7. Predicted Cu superfilling of a trench of aspect ratio 4 for kinetic parameters from Table I for values of D/wv_0 (left to right): 0.01, 0.1, 1, and 10. The predictions correspond to the four points marked in Fig. 6. The trench fails to fill for the two lower values of D/wv_0 (0.01 and 0.1) and successfully fills for the higher values (1.0 and 10). Mobility of the adsorbed accelerator is thus seen to improve filling beyond the range of aspect ratio permitted by the CEAC superfilling mechanism for nonmobile adsorbates. This improvement arises because the resulting variation of the deposits on the sidewalls permits geometrical leveling. For values of D/wv_0 significantly greater than 10, the variation of deposition rate along the sidewall decreases, a trend already evident for $D/wv_0 = 10$, ultimately resulting in conformal filling and a decrease to 0.5 for the maximum aspect ratio that can be filled without seam formation.

filling mechanism and permit meaningful interpretation of filling results (a point that these authors have made before).

Figure 6 predicts filling for some extremely narrow, high-aspect-ratio geometries where transport, were it accounted for, would likely lead to void formation rather than successful filling. Evaluating the (presumably negative) impact of the resulting metal ion depletion on the increased range of filling conditions obtained for nonzero surface mobility is beyond the scope of this paper.

Although not studied here, finite adsorbate diffusion along the deposit surface might be expected to impact stabilization of planar deposits against roughening provided by the CEAC mechanism,^{25,26} a concern for processes that utilize (knowingly or otherwise) such stabilization to obtain smooth deposits.

Conclusions

The CEAC mechanism has been extended to account for diffusion of accelerating adsorbates along the surface of the deposit in response to CEAC-induced gradients of coverage. Results indicate that the disclosed Cu superfill process is not substantially affected by surface mobility of adsorbates, while the disclosed gold superfill process is significantly impacted by adsorbate migration. While no modeling was performed, evidence suggests that the disclosed silver superfill process is also impacted by significant diffusion of the accelerator along the surfaces upon which it is adsorbed. Based on comparison of simulation and experiment, an upper bound was suggested for the diffusion coefficient of adsorbed SPS accelerator in the superfilling Cu electrolyte; approximate values were suggested for the diffusion coefficients for adsorbed Pb accelerator in a superfilling Au electrolyte and adsorbed Se accelerator in a superfilling Ag electrolyte. Modeling predicts a beneficial impact on feature filling of limited adsorbate mobility and a detrimental impact of excessive mobility. While diffusion of accelerating adsorbates along the deposit surface works against enrichment on the bottom surface of filling features through the CEAC mechanism of superfilling, the simulations indicate that limited diffusion can be beneficial for filling because it creates tilted sidewalls compatible with geometrical leveling. The spatial extent of diffusional redistribution of the accelerator from eliminated surface area increases with D/v_0w , resulting in increasing tilt of the sidewall deposits up to and beyond the length scale of the trench height and an associated increase of the aspect ratio that can be filled seam-free. Increase of D/v_0w beyond ≈ 10 leads to redistribution of the displaced accelerator over such a large spatial extent that the gradient of coverage along the sidewall begins

to decrease, causing reduced tilt of the sidewall deposits and a rapid reduction to the 0.5 maximum value expected for seam-free, conformal filling.

Significantly, current-voltage (voltammetry) and current-time (chronoamperometry) metrologies²³ that have been shown to be extremely effective for quantifying the impact of adsorbates on metal deposition rates and adsorbate accumulation and consumption kinetics for prediction of superfilling are not affected by surface diffusion; these metrologies utilize surfaces with uniform coverage of adsorbate. As a result, they are unable to provide guidance on adsorbate mobility. Based on the results presented in this work, it is clear that quantification of such surface transport is already necessary for understanding superconformal, and more specifically, superfilling, processes and will become increasingly important as features continue to shrink.

The National Institute of Standards and Technology assisted in meeting the publication costs of this article.

References

1. P. C. Andricacos, C. Uzoh, J. O. Dukovic, J. Horkans, and H. Deligianni, *IBM J. Res. Dev.*, **42**, 567 (1998).
2. T. P. Moffat, B. Baker, D. Wheeler, J. E. Bonevich, M. Edelstein, D. R. Kelly, L. Gan, G. R. Stafford, P. J. Chen, W. F. Egelhoff, and D. Josell, *J. Electrochem. Soc.*, **149**, C423 (2002).
3. D. Josell, B. Baker, C. Witt, D. Wheeler, and T. P. Moffat, *J. Electrochem. Soc.*, **149**, C637 (2002).
4. B. C. Baker, M. Freeman, B. Melnick, D. Wheeler, D. Josell, and T. P. Moffat, *J. Electrochem. Soc.*, **150**, C61 (2003).
5. B. C. Baker, C. Witt, D. Wheeler, D. Josell, and T. P. Moffat, *Electrochem. Solid-State Lett.*, **6**, C67 (2003).
6. E. J. Ahn and J. J. Kim, *Electrochem. Solid-State Lett.*, **7**, C118 (2004).
7. D. Josell, C. R. Beauchamp, D. R. Kelley, C. A. Witt, and T. P. Moffat, *Electrochem. Solid-State Lett.*, **8**, C54 (2005).
8. D. Josell, D. Wheeler, and T. P. Moffat, *J. Electrochem. Soc.*, **153**, C11 (2006).
9. H. Park, W. Koh, S.-M. Choi, K.-C. Park, H.-K. Kang, J.-T. Moon, K. Shim, H. Lee, O. Kwon, and S. Kang, in *Proceedings of The IEEE 2001 International Technology Conference*, June 4–6, 2001, p. 12 (2001).
10. S. G. Pyo, W. S. Min, H. D. Kim, S. Kim, T. K. Lee, S. K. Park, and H. C. Sohn, in *Advanced Metallization Conference*, Materials Research Society, p. 209 (2001).
11. K.-C. Shim, H.-B. Lee, O.-K. Kwon, H.-S. Park, W. Koh, and S.-W. Kang, *J. Electrochem. Soc.*, **149**, G109 (2002).
12. D. Josell, D. Wheeler, and T. P. Moffat, *Electrochem. Solid-State Lett.*, **5**, C44 (2002).
13. D. Josell, S. Kim, D. Wheeler, T. P. Moffat, and S. G. Pyo, *J. Electrochem. Soc.*, **150**, C368 (2003).
14. O.-K. Kwon, J.-H. Kim, H.-S. Park, and S.-W. Kang, *Electrochem. Solid-State Lett.*, **6**, C109 (2003).
15. K. M. Takahashi and M. E. Gross, *J. Electrochem. Soc.*, **146**, 4499 (1999).

16. M. Georgiadou, D. Veyret, R. L. Sani, and R. C. Alkire, *J. Electrochem. Soc.*, **148**, C54 (2001).
17. A. C. West, *J. Electrochem. Soc.*, **147**, 227 (2000).
18. Y. Cao, P. Taephaisitphongse, R. Chalupa, and A. C. West, *J. Electrochem. Soc.*, **148**, C466 (2001).
19. A. C. West, S. Mayer and J. Reid, *Electrochem. Solid-State Lett.*, **4**, C50 (2001).
20. D. Josell, D. Wheeler, W. H. Huber, and T. P. Moffat, *Phys. Rev. Lett.*, **87**, 016102 (2001).
21. T. P. Moffat, D. Wheeler, W. H. Huber, and D. Josell, *Electrochem. Solid-State Lett.*, **4**, C26 (2001).
22. Z. Hu and T. Ritzdorf, *Electrochem. Solid-State Lett.*, **153**, C467 (2006).
23. T. P. Moffat, D. Wheeler, M. Edelstein, and D. Josell, *IBM J. Res. Dev.*, **49**, 19 (2005).
24. D. Wheeler, D. Josell, and T. P. Moffat, *J. Electrochem. Soc.*, **150**, C302 (2003).
25. G. B. McFadden, S. R. Coriell, T. P. Moffat, D. Josell, D. Wheeler, W. Schwarzscher, and J. Mallett, *J. Electrochem. Soc.*, **150**, C591 (2003).
26. D. Wheeler, T. P. Moffat, G. B. McFadden, S. Coriell, and D. Josell, *J. Electrochem. Soc.*, **151**, C538 (2004).